Lab on a Chip

PAPER

View Article Online
View Journal | View Issue

Cite this: *Lab Chip*, 2021, **21**, 888

Sequential capillarity-assisted particle assembly in a microfluidic channel†

Roberto Pioli,[a] Miguel Angel Fernandez-Rodriguez,[bc] Fabio Grillo,[b] Laura Alvarez,[b] Roman Stocker,[a] Lucio Isa *[b] and Eleonora Secchi *[a]

Received 23rd September 2020,
Accepted 22nd December 2020

DOI: 10.1039/d0lc00962h

rsc.li/loc

Colloidal patterning enables the placement of a wide range of materials into prescribed spatial arrangements, as required in a variety of applications, including micro- and nano-electronics, sensing, and plasmonics. Directed colloidal assembly methods, which exploit external forces to place particles with high yield and great accuracy, are particularly powerful. However, currently available techniques require specialized equipment, which limits their applicability. Here, we present a microfluidic platform to produce versatile colloidal patterns within a microchannel, based on sequential capillarity-assisted particle assembly (sCAPA). This new microfluidic technology exploits the capillary forces resulting from the controlled motion of an evaporating droplet inside a microfluidic channel to deposit individual particles in an array of traps microfabricated onto a substrate. Sequential depositions allow the generation of a desired spatial layout of colloidal particles of single or multiple types, dictated solely by the geometry of the traps and the filling sequence. We show that the platform can be used to create a variety of patterns and that the microfluidic channel easily allows surface functionalization of trapped particles. By enabling colloidal patterning to be carried out in a controlled environment, exploiting equipment routinely used in microfluidics, we demonstrate an easy-to-build platform that can be implemented in microfluidics labs.

Introduction

Particle assembly as a method for the fabrication of complex patterns with programmable geometries and compositions has experienced significant expansion in recent years. This interest stems from the wide range of applications where miniaturization plays an important role, including micro- and nano-electronics,[1,2] sensing,[3] and plasmonics.[4,5] The working principle consists in using nano- and micro-particles as building blocks for the construction of more complex structures across length scales, from the colloidal scale upward. Directly using particles for pattern formation offers significant advantages compared to top-down patterning techniques. In particular, progress in the synthesis of functional nano- and microparticles offers a vast library of preformed units and their combination grants greater flexibility compared to patterning metallic, oxide or polymeric films, for example *via* lithography. Additionally, colloidal particles can be synthesized out of diverse materials and easily modified to exhibit specific surface chemistries. Producing colloidal patterns by co-localizing particles with different bulk or surface properties in prescribed positions offers tantalizing opportunities to create chemical patterns with selective binding properties, which can be directly employed in surface-based sensing. In contrast, achieving top-down micropatterns encoding different functionalizations requires complex sequential or multiplexing processes,[6] necessitating sophisticated equipment, delicate alignment and protection procedures.

In the field of particle assembly, several approaches have been proposed to create heterogeneous patterns, including self-assembly,[7,8] pick-and-place methods,[9] and directed assembly.[10–12] In self-assembly techniques, controlled interactions between particles are exploited to create ordered structures. Their main limitation lies in the fact that efficiency is strongly dependent on the operating conditions,[13] as well as on the specific properties of the particles, which define their mutual interactions and the interactions with the substrate. This sensitivity often precludes the high yield, reproducibility, and precision required for many applications, such as micro-electronics. Pick-and-place methods, like optical tweezers, enable high precision in particle assembly and the formation of complex structures with great accuracy. However,

[a] *Institute of Environmental Engineering, Department of Civil, Environmental and Geomatic Engineering, ETH Zürich, Stefano-Franscini-Platz 5, 8093 Zürich, Switzerland. E-mail: esecchi@ethz.ch*
[b] *Laboratory for Soft Materials and Interfaces, Department of Materials, ETH Zürich, Vladimir-Prelog-Weg 5, 8093 Zürich, Switzerland. E-mail: lucio.isa@mat.ethz.ch*
[c] *Laboratory of Surface and Interface Physics, Biocolloid and Fluid Physics Group, Faculty of Sciences, University of Granada, Campus de Fuentenueva s/n, ES 18071 Granada, Spain*

† Electronic supplementary information (ESI) available. See DOI: 10.1039/d0lc00962h

this precision comes with high cost and limited yield. Directed assembly instead exploits the action of one or more external forces to guide the organization of colloidal particles into complex structures, with high yield and accuracy, yet rapidly and at limited cost.

Sequential capillarity-assisted particle assembly (sCAPA) is a promising directed assembly technology developed in recent years, with great potential as a patterning tool to allow the co-localization of different micro- and nanoparticles in precisely defined arrangements.[14,15] This technology, derived from conventional capillary assembly,[16,17] exploits the capillary forces exerted by the meniscus of an evaporating droplet of a colloidal suspension that moves over a patterned template, generally made of polydimethylsiloxane (PDMS), to deposit and trap single particles inside microfabricated wells. The evaporation drives the accumulation of particles close to the meniscus, whereby capillarity enforces their placements in the prescribed positions. The capillary forces used in the assembly process[15] act on a larger length scale than those characterizing the interactions between particles, so the success of the deposition is largely independent of the material, dimensions and surface properties of the particles. The yield of the depositions solely depends on global parameters such as particle concentration (up to 1% vol), deposition speed (of the order of few micrometres per second), temperature (between 10 and 50 K above the dew-point temperature) and surface tension of the suspension (*i.e.* leading to the formation of a receding contact angle on the substrate between 30 and 60°).[15,17] This affords great versatility and allows the fabrication of complex colloidal structures, whose shape is determined by the geometry of the traps and whose composition is defined by the assembly sequence. Virtually any kind of colloidal particles forming a stable aqueous suspension can be deposited, comprising different surface charges, and functionality (*e.g.* magnetic), shape (including anisotropic shapes such as nanorods,[21,22] nanopolygons[23,24] and nanowires[1]) and from a broad range of materials including polymers, oxides, metals semiconductors and biological samples.[12] Diverse geometries, ranging from linear sequences to planar clusters such as triangles and L-shaped sequences, can be obtained by using several sequential depositions, with the possibility to change the direction of motion of the meniscus to change the direction of deposition.[14]

The main disadvantage of current implementations of the sCAPA technology is that the process is carried out in an open system. This means that the colloidal suspensions and the patterned substrate are exposed to the surrounding environment, thereby introducing a risk of contamination, which is particularly detrimental for example in sensing applications and for biological samples.[18–20] In addition, a highly customized setup is currently required: the droplet motion is driven by a high-precision piezoelectric stage, mounted on a thermal control module, integrated on a light microscope. In order to avoid contamination issues and facilitate the implementation of the technique, we have developed a simple microfluidic platform to perform sCAPA within a closed microchannel. This versatile and robust platform not only allows the colloidal patterning to be carried out in a controlled environment, but also exploits the same equipment routinely used in microfluidics, simplifying adoption and expanding the range of possible applications.

Materials and methods

Colloidal suspensions

Colloidal patterning experiments were performed using fluorescent polystyrene (PS) particles (microParticles GmbH) of diameter 0.98 μm (red; polydispersity <5%), 1.02 μm (green; polydispersity <5%) and 2 μm (green; red; polydispersity <5%), and polystyrene particles with covalently bound streptavidin on the surface (Micromer® 01–19-203; Micromod Partikeltechnologie GmbH) of diameter 2 μm. To wash particles before use, particle suspensions were diluted with an aqueous solution of TWEEN 20 (Sigma Aldrich; 0.015% v/v) to a final concentration of 0.1% v/v and centrifuged at 12 000 rpm for 1 min. The supernatant was then gently removed with a pipette and replaced with an aqueous solution of TWEEN 20 (Sigma Aldrich; 0.015% v/v). This procedure was repeated three times to ensure complete replacement of the supplier's solvent. All suspensions used for particle assembly had a particle concentration of 0.1% v/v and TWEEN 20 concentration of 0.015% v/v. This surfactant concentration enables an optimal receding contact angle between 30° and 60° during deposition (ESI,† Fig. S1). As proof of concept for *in situ* surface functionalization, polystyrene particles with covalently bound streptavidin on the surface (Micromer® 01–19-203; Micromod Partikeltechnologie GmbH) were exposed to fluorescent biotin using a solution of 10 μM biotin dye (Atto 520-Biotin, Merck) in 10 mM PBS buffer (Gibco PBS pH 7.4 (1×)).

Template fabrication

The PDMS templates, which bear microfabricated traps to form the template for particle deposition, were fabricated according to the method introduced by Geissler *et al.*[25] The silicon master was prepared by conventional lithography[25] in a cleanroom (Binnig and Rohrer Nanotechnology Center, class 100). Features were designed in the open-source software Klayout. A chrome-glass mask with a layer of positive photoresist (AZ1505, MicroChemicals) was prepared by exposing the designed features with a UV direct laser writer (Heidelberg DWL 2000) and developed with a spin developer (OPTIspin SB20) using AZ400K developer (MicroChemicals) at 1:4 photoresist to water ratio for 15 s, then immersed in chrome etchant for 50 s (Techni Etch Cr01, Technic France). A 10 cm silicon wafer (N/Phos <100> 1–10 Ω cm, silicon materials) was plasma treated for 3 min at 600 W (Gigabatch 310 M PVA TePla) and a layer of hexamethyldisilazane was vapor-deposited and baked at 110 °C to increase the adhesion towards the photoresist. A layer of AZ1505 photoresist was then deposited at 2000 rpm for 2 min and the features were exposed to UV through the chrome-glass mask with a

mask aligner (Süss MA6) at 20 mJ for 2 s and developed with AZ400K developer as for the mask. To complete the fabrication of the silicon master, the wafer was etched *via* deep reactive ion exchange (Alcatel AMS 200SE I-Speeder) adjusting the etching time (<2 min) to achieve the desired depth (measured with a profilometer; Veeco Dektak 6 M). To prepare the particle deposition template, polydimethylsiloxane (PDMS; Sylgard 184 silicone elastomer kit, Dow Corning, Midland, MI) was mixed with cross-linker (10% by weight) and degassed, then 3 g was poured onto the silicon master. To obtain a 400 μm-thick layer, PDMS was spin coated at 500 rpm for 5 s and at 800 rpm for 10 s, then degassed again to remove trapped air bubbles. The silicon wafer was baked at 70 °C for 2 h, after which the PDMS template layer was peeled off and was ready to be bonded to the PDMS channel. The templates used for colloidal patterning had dimensions of 10 mm × 5 mm, accommodating ~10^6 traps. Traps large enough to accommodate two adjacent particles were 2 μm long, 1 μm wide, and 500 nm deep (Fig. 3A) for the green and red PS particles of 1.02 μm diameter, and 4 μm long, 2 μm wide, and 1 μm deep (Fig. 3B) for the green and red particles of 2 μm diameter. Traps large enough to accommodate three adjacent particles (Fig. 3C), or two particles at the extremities of the traps (Fig. 3D), were 4 μm long, 1 μm wide, and 500 nm deep, for the green and red PS particles of 1.02 μm diameter. The separation between the traps is at least twice greater than the width of the trap along the direction of the moving meniscus, to ensure that the contact line sequentially dewets traps within a single row and that different rows are sequentially

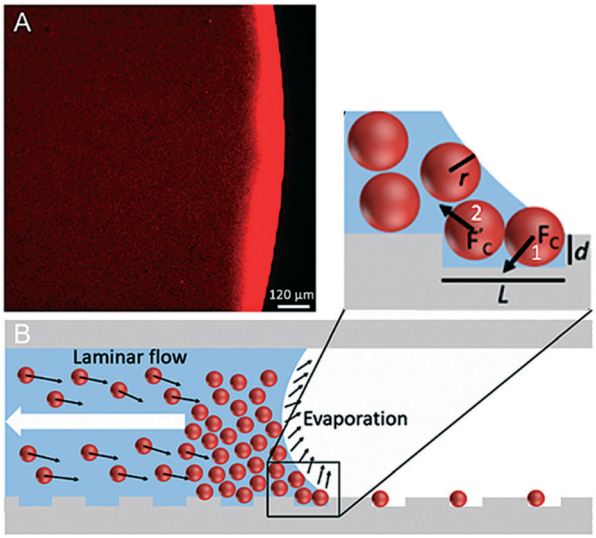

Fig. 2 Working principle of particle deposition in a trap. (A) Fluorescence image showing a top view of a droplet of a colloidal suspension moving (right to left) on the PDMS template. The brighter region is the particle accumulation zone. (B) Schematic of particle assembly in rectangular traps and magnified view of one trap. The trap depth d is of the same order as the particle radius r. The meniscus exerts on the front particle (particle 1) a capillary force F_C that is oriented perpendicularly to the meniscus itself, thus pushing the particle into the trap and to the end of the trap towards which the meniscus is moving (here, the left end). The force F_C is partially transmitted to the rear particle (particle 2), resulting in an upward force F'_C that pushes particle 2 out of the trap. As a result, only particle 1 is deposited within the trap.

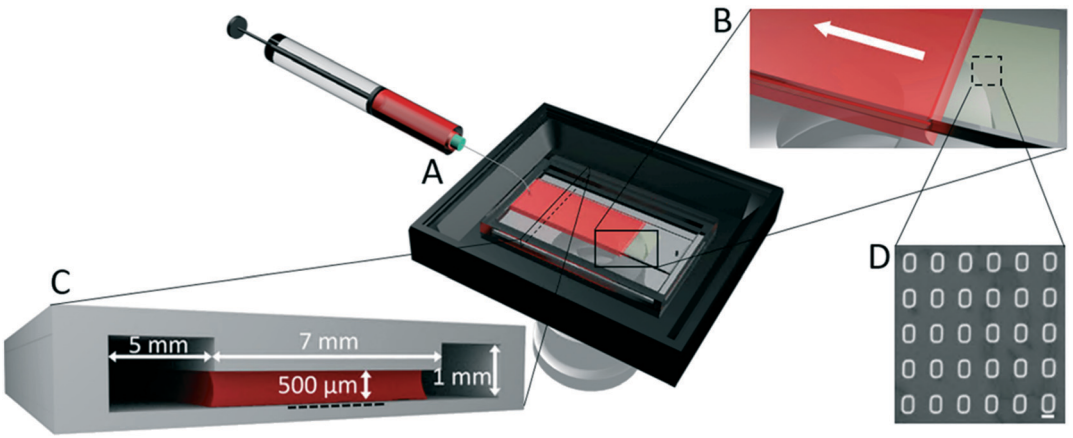

Fig. 1 Microfluidic sequential capillarity-assisted particle assembly (microfluidic sCAPA) platform. (A) Schematic of the experimental setup for microfluidic sCAPA. The system consists of a thermal control chamber (in black) in which the 23 mm long microfluidic channel is placed, set on top of an inverted microscope stage (see objective below the chamber). A syringe controlled by a syringe pump (not shown) is first used to inject the colloidal suspension (from left to right into the channel), and then is operated to withdraw it (from right to left) during the deposition process. The floor of the microfluidic channel includes a region with the microfabricated traps (*i.e.* the template), as shown in D. The red shading represents the colloidal suspension. (B) Magnified side-view of the meniscus moving in the central part of the channel while withdrawn using the syringe pump. The arrow shows the direction of the meniscus movement. The dashed square indicates the location of the template, as magnified n D. (C) Cross-section of the PDMS microfluidic channel. The geometry of the ceiling defines three sections: a central one that is 7 mm wide and 500 μm high, and two lateral ones that are each 5 mm wide and 1 mm high. The template is located on the channel's floor, underneath the central section (represented by a dashed line in the figure). Through suction from the syringe, the colloidal suspension is made to recede in the central section of the microchannel, eliciting deposition of particles into the traps, while the two lateral sections are filled with air for the entire time, to ensure that the colloidal suspension does not get in contact with the channel's walls. (D) SEM image of a small portion of the PDMS template showing 36 microfabricated rectangular (2 μm × 4 μm) traps. The scale bar is 2 μm. The overall size of the template area is 50 mm^2.

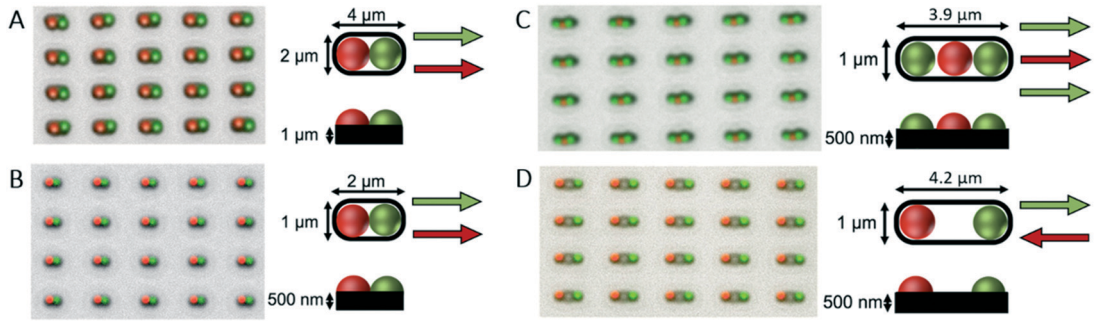

Fig. 3 Colloidal arrays assembled with the microfluidic sCAPA. (A and B) Epifluorescence microscopy image of 20 traps showing dimers assembled from one green and one red polystyrene particles of diameter 2 μm (A) and 1 μm (B) along with the deposition schematics. Arrows show the direction of meniscus movement for each deposition step. (C) Epifluorescence microscopy image of 20 traps showing trimers assembled from two green and one red polystyrene particles of diameter 1 μm along with the deposition schematics. (D) Epifluorescence microscopy image of 20 traps showing the deposition of one green and one red polystyrene particles of diameter 1 μm, separated by roughly 2 μm, obtained by alternating the direction of the meniscus movement between the two deposition steps.

dewetted, in order to maintain a well-controlled motion of the meniscus.

Channel fabrication

PDMS channels were fabricated by pouring PDMS onto an aluminum mold and curing at 70 °C for 2 h. Fig. 1C shows the cross-section of the channel. It consists of three 23 mm long parallel sections. The two side sections are each 5 mm wide, and 1 mm high, and the central section is 7 mm wide and 500 μm high. There is no physical barrier between the three sections. The shallowest part of the microfluidic channel is located above the template, namely, the region of the channel floor bearing the microfabricated traps. The two parts of the microfluidic channel (ceiling and floor) can be plasma bonded (40 s plasma treatment with a Zepto Plasma Unit, Diener electronic GmbH), or held together using external clamps. Both sealing strategies were successfully tested.

Particle patterning

The experimental setup used for the particle patterning consists of the microfluidic channel, a syringe pump, and a thermal control module (Fig. 1A). The colloidal suspension is injected into the microfluidic channel, through a hole punched at the beginning of the middle section, while the hole at the other end of the channel allows air to escape. Once the liquid has covered the template region that sits on the bottom of the channel (see the supporting information for details of the filling procedure), it is withdrawn and, once the accumulation zone (as defined later) is formed, particles start being deposited. The liquid withdrawal speed of the syringe pump (CETONI Base 120, CETONI GmbH) was set at a flow rate such that the meniscus moves at a constant speed of 1–2 μm s^{-1} during deposition. The control module, a heated glass plate equipped with a controller (H601-NIKON-TS2R-GLASS and H401-T-CONTROLLER, Okolab), is placed below the microfluidic channel to maintain a temperature of 27–30 °C. The thermal control module allows full optical access and the assembly can be visualized in real time with an inverted microscope (Nikon Eclipse Ti).

Imaging and data analysis

Particles assembled in the traps were imaged by bright field and fluorescence optical microscopy (Nikon Eclipse Ti). ImageJ[26] was used to merge the fluorescence images, and to overlay fluorescence and bright-field images by combining the red, green, and phase contrast channels. The yield of the assembly steps was quantified by particle localization and cluster analysis using a custom-made routine implemented in Matlab. Microscopy images of a target region of the template containing >50 000 traps were taken after each deposition step with fluorescence optical microscopy using either the red or the green channel to discern particles assembled during each step. Particles of different fluorescence were then located in the different images using Matlab code to calculate the position of centroids of bright spots to sub-pixel accuracy.[27,28] The particle coordinates were then tagged and collated according to the fluorescence channel used to acquire the image. The Matlab routine *rangesearch* was used to construct the list of nearest neighbours of each particle based on a cut-off Euclidean distance of $r \leq 1.4\sigma$, where σ is the diameter of the particles. The list of nearest neighbours was then used to find and classify clusters of particles separated by distances less than r.

Results and discussion

The setup for the microfluidic sCAPA consists of a microfluidic channel, in which a colloidal suspension is moved by a syringe pump and the temperature is controlled by a commercial thermal control module. This simple microfluidic setup can be mounted on any microscope. The template for deposition is located below the central section of the microfluidic platform (Fig. 1). An important element of the device is the shape of the microchannel's cross-section, with the height of the central section being half that of the lateral sections (Fig. 1C). In this manner, after being injected, the

liquid is pinned by the sharp edges of the central section of the channel and consequently confined, leaving air in the lateral sections. This design allows the maintenance of a well-defined moving droplet with a receding convex-shaped meniscus. In particular, the presence of the lateral air pockets prevents contact of the meniscus with the side walls, which would generate a concave-shaped meniscus with a non-reproducible shape.

The colloidal suspension is injected into the microfluidic device through an inlet located in the upstream part of the central section, until the solution covers the template region containing the microfabricated traps. At the downstream end of the channel, an outlet allows air to escape during the liquid injection process. Thanks to the different height profile of the channel, the particle suspension remains trapped in the central, thinner section by surface tension, which prevents it from spreading over into the lateral air reservoirs. Being pinned in the central section, the suspension proceeds with a convex-shaped meniscus until it reaches the end of the channel (ESI† Fig. S2). Once the template has been covered by the colloidal suspension (see ESI† for details of the filling procedure), the syringe pump is used to withdraw the liquid at a flow rate of 0.07–0.2 μl min^{-1}, corresponding to a meniscus receding speed of 1–2 μm s^{-1}. The channel's upstream-downstream symmetry facilitates the inversion of the patterning direction between patterning steps (inlet becomes outlet, and *vice-versa*).

Throughout the process, the receding liquid evaporates at a controlled temperature, causing convective currents to carry the suspended particles towards the air–liquid interface, as in the classic sCAPA technique.[14,15] The region surrounding the air-liquid interface, called the accumulation zone, is thus characterized by a high concentration of particles. The particles concentrated in the accumulation zone, starting from those at the air–liquid interface in immediate contact with the template, get deposited into the traps as the liquid recedes (Fig. 2B), owing to the capillary force pushing the particles into the traps.[15] Since the accumulation zone is formed by evaporation, the accumulation rate and consequently the size of this zone can be controlled by regulating the temperature within the channel. The higher the temperature, the greater the size of the accumulation zone and the faster its formation, due to the higher speed of the convective currents. Increasing the particle concentration beyond 1% vol may lead to the formation of a too large, poorly controlled accumulation zone even at moderate heating, causing a drop in the deposition yield. The temperature in the whole channel must be maintained above the dew point of water in order to avoid condensation on the template (ESI,† Fig. S2). This can be achieved by maintaining the temperature in the whole channel at 27 °C to 30 °C, approximately 15 °C above the dew point of water. The desired wetting conditions of the template (*i.e.*, a receding contact angle[15] between 30° and 60°) can be achieved by modulating the surfactant concentration. We found that a concentration of 0.015% TWEEN 20 made for a 46.0 ± 3.8° receding contact angle (ESI† Fig. S1C) and allowed the reliable deposition of both 1 μm and 2 μm diameter fluorescent polystyrene (PS) particles (microParticles GmbH).

The microfluidic platform can be used to create patterns of particles with different geometries, depending on the shape and arrangement of the traps. The number of particles that are pushed into the traps in each deposition can be controlled by the geometry of the traps and the flow direction. Here, we demonstrate the assembly of different linear patterns of particles, obtained through sequential deposition steps within traps having a width close to the particle diameter and different lengths, and oriented such that the motion of the meniscus occurred along the direction of the long axis of the traps. This technique achieves a yield up to 95% for each individual step, where the yield is defined by the percentage of the traps on the template where the desired number of particles is successfully deposited. For each experiment, the yield was quantified by imaging at 40× magnification, using both bright-field and fluorescence microscopy, and automatically counting particles with a custom-written Matlab software. The yields and the flexibility in the designs reported below are on par with what can be achieved by conventional sCAPA in an open chip.[14,15]

We started by creating particle dimers by running the microfluidic sCAPA process twice, sequentially. We first injected a colloidal suspension of green fluorescent polystyrene particles with diameter of 2 μm through the inlet into the central section of the channel, using a manually operated syringe, until the template was fully covered. We then withdrew the suspension out of the microchannel's outlet using the syringe pump, at a flow rate of 0.1 μl min^{-1} to deposit one particle per trap. Once the suspension reached the end of the template, we completely withdrew the suspension of green polystyrene particles, injected a suspension of red fluorescent polystyrene particles with 2 μm diameter and repeated the same deposition procedure. This resulted in the formation of green–red (G–R) dimers (Fig. 3A). The desired G–R dimers formed in 93% of the approximately 55 000 analysed traps. This experiment demonstrates that the conditions for a successful sCAPA can be achieved within the enclosed space of a microfluidic channel. In particular, the formation of a sufficiently large accumulation zone, with a width ranging from 100 μm to 300 μm, can be realized, which results in a high yield of particles deposited in the traps according to a prescribed sequence, as mentioned above. In a second set of experiments, we demonstrated that the process works also for smaller particles using red and green polystyrene particles with diameter of 1 μm to form green–red (G–R) dimers (Fig. 3B) with similar results. In this case, G–R dimers were deposited in 89% of the approximately 55 000 analysed traps. For both experiments, 1 cm long templates containing approximately 10^6 traps can be filled in under 2.5 hours.

More complex patterns can also be achieved, for example longer, bar-code-like colloidal chains. To illustrate this, we produced G–R–G chains using a three-step process (Fig. 3C).

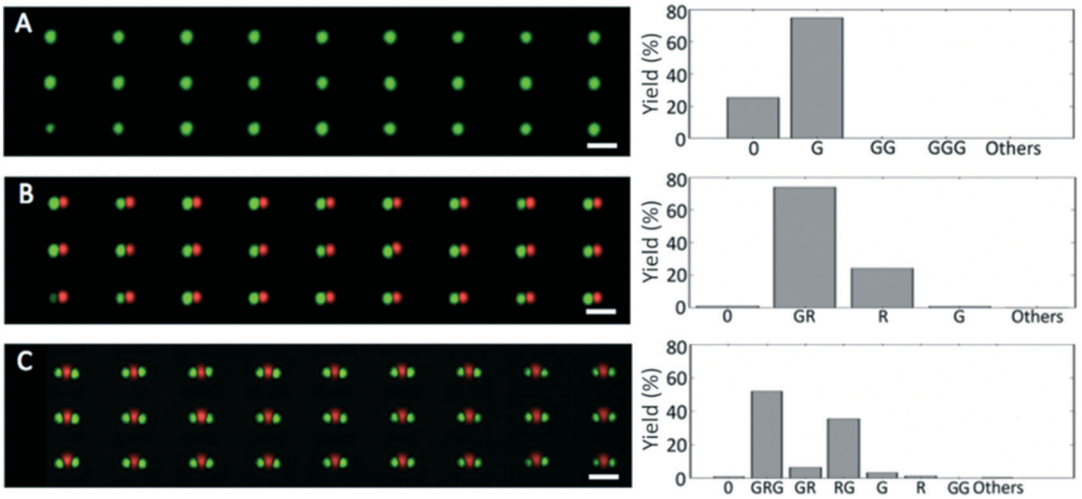

Fig. 4 Sequential depositions for the formation of a two-dimensional colloidal array of particle trimers using microfluidic sCAPA. (A) One-step deposition of fluorescent green polystyrene particles of diameter 1 μm, in linear traps like those in Fig. 3C. The yield of single green particles is 75%. (B) Two-step deposition of fluorescent red polystyrene particles of diameter 1 μm in the traps containing the fluorescent green polystyrene particles from the previous step. The yield of the desired green–red sequence is 74%. (C) Three-step deposition of fluorescent green particles of diameter 1 μm in the traps containing the green and the red particles from the previous steps. The yield of the desired green–red–green sequence is 52%. Scale bars in A–C are 4 μm. The histograms show the relative frequency of the different particle combinations measured for approximately 55 000 traps for each deposition type. In ESI† Table S1, the yield of each deposition step is reported.

Specifically, we added a third deposition step to the process for the dimer fabrication, thereby demonstrating that this platform can be used to pattern sequences of several particles by performing multiple depositions in series. For the three-particle linear chains, the yield of the deposition of the first (green) and the second (red) particles were 75% (41 240 traps over 55 144 filled with a G particle) and 74% (40 706 traps over 55 144 filled with a G–R sequence), respectively. After the third deposition, G–R–G sequences were present in 52% of the analyzed traps and dimers consisting of a red and a green particle (R–G) amounted to 36% (Fig. 4). The overall number of the G–R–G trimers produced over the 55 000 traps that we imaged after the three depositions was greater than 28 000. We again remark that the full 10 mm × 5 mm template accommodates approximately 10^6 traps, hence, given a yield of 52%, more than 500 000 trimers can be readily fabricated in parallel using this approach. The deposition yields of each particle types give analogous results and are compatible with the outcome of the standard process with open samples.[14]

Precise positioning is also possible without contact between the particles. We demonstrated this by placing two particles of 1 μm diameter (one red, one green) at the opposite ends of 4 μm long linear traps (Fig. 3D). In this case, the two sequential depositions were performed in opposite directions, with the green particles deposited while the liquid was receding in one direction, and the red ones deposited while the liquid was receding in the opposite direction. By manipulating the trap design and the direction of deposition, this method therefore allows one to control not only the sequence of deposition, but also the separation between deposited particles.

The technique can be also used to selectively apply chemical patterns to surfaces with micrometric precision, exploiting the controlled location of the trapped particles. As a proof of concept, we patterned a surface with biotin dye, which binds to streptavidinylated molecules. We first deposited non-fluorescent polystyrene particles with covalently bound streptavidin on their surface (Fig. 5A). After deposition, we filled the microfluidic channel with a solution of green fluorescent biotin dye (containing 10 μM Atto 520-Biotin and 10 mM PBS), to allow it to bind to the streptavidinylated molecules. The solution was left in the channel for 10 h and then flushed out with water to image the template. Before filling the channel with the biotin dye solution, the particles did not show any fluorescence. After exposure to the fluorescent biotin-conjugated dye, the selective binding between fluorescent biotin and streptavidin on the particles' surface made them fluorescent (Fig. 5 – see ESI† Fig. S4 for a control experiment with unfunctionalized particles). This experiment shows the ability of the technique to precisely pattern molecules in specific locations defined by the position of trapped particles presenting given surface chemistries.

Conclusions

We have developed a microfluidic sCAPA platform that permits the assembly of colloidal particles in a microfluidic channel and the use of the deposited particles to create a chemical pattern over a target surface. This constitutes a leap forward for capillary assembly, in particular for sCAPA, allowing the approach to retain the original advantages in terms of yield and patterning flexibility, but to benefit from

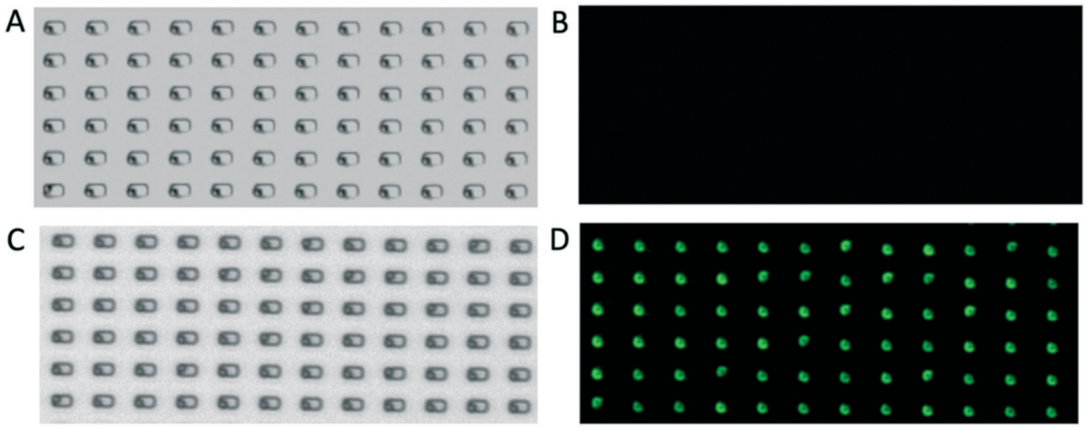

Fig. 5 Surface patterning of trapped streptavidin-functionalized particles with a biotin fluorescent dye. (A and B) Bright-field (A) and epi-fluorescence (B) image of a section of the PDMS template after a single deposition of polystyrene particles (2 μm diameter) with covalently bound streptavidin on the surface. (C and D) Bright-field (C) and epifluorescence (D) image of the same PDMS template section, after filling the microfluidic channel with a biotin fluorescent dye solution. The biotin molecules bind to streptavidin covalently bound to the particles' surface, making the particles fluorescent.

the use of standard microfluidics operating conditions. Particle assembly within a closed channel is, in particular, advantageous in reducing the risk of contamination and opens up a broad range of possibilities to post-functionalize the deposited particle patterns by means of controlled flows in a single microfluidic device. These advantages overcome the current limitations of open sCAPA chips, where embedding the deposited patterns within closed channels would require difficult handling of the substrates, *e.g.* for channel bonding and sealing. Thanks to the high throughput inherent in the technique, the ability to position particles on a template with micrometric precision, and the prevention of contamination, microfluidic sCAPA opens new and unexplored possibilities in the field of surface patterning.

Authors contribution

Author contributions are defined based on the CRediT (contributor roles taxonomy) and listed alphabetically. Conceptualization: L. A. F., M. A. F. R., L. I., R. P., E. S., R. S. Data curation: R. P., E. S. Formal analysis: R. P. Funding acquisition: L. I., E. S., R. S. Investigation: R. P., E. S. Methodology: L. A. F., M. A. F. R., L. I., R. P., E. S. Project administration: L. I., E. S., R. S. Resources: M. A. F. R., E. S., R. S. Software: F. G. Supervision: L. I., E. S., R. S. Validation: L. A. F., M. A. F. R., F. G., R. P. Visualization: F. G., L. I., R. P., E. S. Writing – original draft: L. I., R. P., E. S. Writing – review and editing: L. I., R. P., E. S., R. S.

Conflicts of interest

There are no conflicts to declare.

Acknowledgements

The authors acknowledge support from an ETH Research Grant ETH-15 17-1 (R. S.), from an ETH Postdoctoral Fellowship FEL-21 15-2 and SNSF PRIMA Grant 179834 (E. S.), from a Postdoctoral fellowships programme "Beatriu de Pinós", funded by the Secretary of Universities and Research (Government of Catalonia) and by the Horizon 2020 programme of research and innovation of the European Union under the Marie Sklodwoska-Curie grant agreement no. 801370 (Grant 2018 BP 00029) (M. A. F. R.) and from a Gordon and Betty Moore Foundation Investigator Award on Aquatic Microbial Symbiosis (grant GBMF9197) (R. S.).

The authors thank Dr. Heiko Wolf at IBM Research Zurich for insightful discussions.

References

1 M. Collet, S. Salomon, N. Y. Klein, F. Seichepine, C. Vieu, L. Nicu and G. Larrieu, *Adv. Mater.*, 2015, **27**, 1268–1273.
2 A. Rey, G. Billardon, E. Lörtscher, K. Moth-Poulsen, N. Stuhr-Hansen, H. Wolf, A. Stemmer and H. Riel, *Nanoscale*, 2013, **5**, 8680–8688.
3 V. Liberman, C. Yilmaz, T. M. Bloomstein, S. Somu, Y. Echegoyen, A. Busnaina, S. G. Cann, K. E. Krohn, M. F. Marchant and M. Rothschild, *Adv. Mater.*, 2010, **22**, 4298–4302.
4 N. J. Greybush, M. Saboktakin, X. Ye, C. Della Giovampaola, S. J. Oh, N. E. Berry, N. Engheta, C. B. Murray and C. R. Kagan, *ACS Nano*, 2014, **8**, 9482–9491.
5 J. A. Fan, K. Bao, L. Sun, J. Bao, V. N. Manoharan, P. Nordlander and F. Capasso, *Nano Lett.*, 2012, **12**, 5318–5324.
6 G. Csucs, R. Michel, J. W. Lussi, M. Textor and G. Danuser, *Biomaterials*, 2003, **24**, 1713–1720.
7 E. V. Shevchenko, D. V. Talapin, N. A. Kotov, S. O'Brien and C. B. Murray, *Nature*, 2006, **439**, 55–59.
8 F. Li, D. P. Josephson and A. Stein, *Angew. Chem., Int. Ed.*, 2011, **50**, 360–388.
9 M. C. Zhong, A. Y. Liu and R. Zhu, *Appl. Sci.*, 2018, **8**, 1522.

10 B. D. Smith, T. S. Mayer and C. D. Keating, *Annu. Rev. Phys. Chem.*, 2012, **63**, 241–263.
11 A. F. Demirörs, *J. Phys. Chem. B*, 2016, **120**, 9759–9765.
12 S. Ni, L. Isa and H. Wolf, *Soft Matter*, 2018, **14**, 2978–2995.
13 Z. Nie, D. Fava, E. Kumacheva, S. Zou, G. C. Walker and M. Rubinstein, *Nat. Mater.*, 2007, **6**, 609–614.
14 S. Ni, J. Leemann, I. Buttinoni, L. Isa and H. Wolf, *Sci. Adv.*, 2016, **2**, e1501779.
15 S. Ni, J. Leemann, H. Wolf and L. Isa, *Faraday Discuss.*, 2015, **181**, 225–242.
16 Y. Yin, Y. Lu, B. Gates and Y. Xia, *J. Am. Chem. Soc.*, 2001, **123**, 8718–8729.
17 L. Malaquin, T. Kraus, H. Schmid, E. Delamarche and H. Wolf, *Langmuir*, 2007, **23**, 11513–11521.
18 L. Chopinet, C. Formosa, M. P. Rols, R. E. Duval and E. Dague, *Micron*, 2013, **48**, 26–33.
19 E. Dague, E. Jauvert, L. Laplatine, B. Viallet, C. Thibault and L. Ressier, *Nanotechnology*, 2011, **22**, 395102.
20 C. Formosa, F. Pillet, M. Schiavone, R. E. Duval, L. Ressier and E. Dague, *Nat. Protoc.*, 2015, **10**, 199–204.
21 V. Flauraud, M. Mastrangeli, G. D. Bernasconi, J. Butet, D. T. L. Alexander, E. Shahrabi, O. J. F. Martin and J. Brugger, *Nat. Nanotechnol.*, 2017, **12**, 73–80.
22 C. Kuemin, L. Nowack, L. Bozano, N. D. Spencer and H. Wolf, *Adv. Funct. Mater.*, 2012, **22**, 702–708.
23 Y. Zhou, X. Zhou, D. J. Park, K. Torabi, K. A. Brown, M. R. Jones, C. Zhang, G. C. Schatz and C. A. Mirkin, *Nano Lett.*, 2014, **14**, 2157–2161.
24 J. Henzie, S. C. Andrews, X. Y. Ling, Z. Li and P. Yang, *Proc. Natl. Acad. Sci. U. S. A.*, 2013, **110**, 6640–6645.
25 M. Geissler, H. Wolf, R. Stutz, E. Delamarche, U. W. Grummt, B. Michel and A. Bietsch, *Langmuir*, 2003, **19**, 6301–6311.
26 J. Schindelin, I. Arganda-Carreras, E. Frise, V. Kaynig, M. Longair, T. Pietzsch, S. Preibisch, C. Rueden, S. Saalfeld, B. Schmid, J. Y. Tinevez, D. J. White, V. Hartenstein, K. Eliceiri, P. Tomancak and A. Cardona, *Nat. Methods*, 2012, **9**, 676–682.
27 J. C. Crocker, D. G. Grier and J. Colloid Interface, *Sci.*, 1996, **179**, 298.
28 D. Blair and E. Dufresne, *MATLAB Particle Tracking*, Georgetown Physics, 2008.